

0

PB82-203720

On the Off-Axis Tensile Test for
Unidirectional Composites

SDTIC
ELECTR
JAN 25 1995
C

Virginia Polytechnic Inst. and State Univ.
Blacksburg

Prepared for

National Aeronautics and Space Administration
Hampton, VA

Apr 82

19951228 067

DEPARTMENT OF DEFENSE
PLASTICS TECHNICAL EVALUATION CENTER
WRIGHT-PATTERSON AIR FORCE BASE, OHIO

PLASTED
43590

U.S. Department of Commerce
National Technical Information Service

NTIS

DISTRIBUTION STATEMENT A
Approved for public release
Distribution Unlimited

Date: 7/15/95 Time: 6:17:57PM

Page: 1 Document Name: untitled

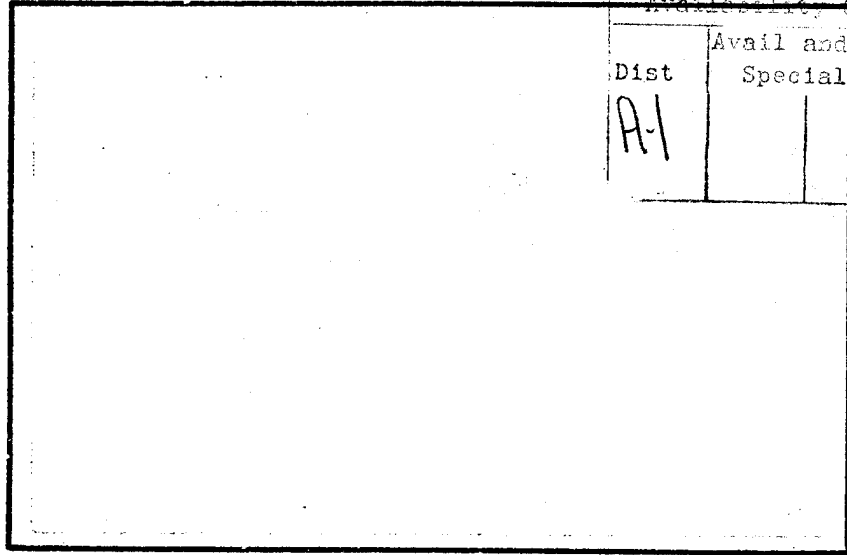
1 OF 2

DTIC DOES NOT HAVE THIS ITEM

-- 1 - AD NUMBER: D436141
-- 5 - CORPORATE AUTHOR: VIRGINIA POLYTECHNIC INST AND STATE UNIV
-- BLACKSBURG DEPT OF ENGINEERING SCIENCE AND MECHANICS
-- 6 - UNCLASSIFIED TITLE: ON THE OFF-AXIS TENSILE TEST FOR
-- UNIDIRECTIONAL COMPOSITES.
--10 - PERSONAL AUTHORS: NEMETH, M. P. ; HERAKOVICH, C. T. ; POST, D. ;
--11 - REPORT DATE: APR , 1982
--12 - PAGINATION: 30P
--14 - REPORT NUMBER: VPI-E-82-9, IR-20
--15 - CONTRACT NUMBER: NCC1-15, ENG-78-24609
--18 - MONITOR ACRONYM: NASA
--19 - MONITOR SERIES: CR-168853
--20 - REPORT CLASSIFICATION: UNCLASSIFIED
--22 - LIMITATIONS (ALPHA): APPROVED FOR PUBLIC RELEASE; DISTRIBUTION
-- UNLIMITED. AVAILABILITY: NATIONAL TECHNICAL INFORMATION SERVICE,
-- SPRINGFIELD, VA. 22161. N82-23553.
--33 - LIMITATION CODES: 1 24

**OF COLLEGE
ENGINEERING**

Accession For		
NTIS GRA&I	<input checked="" type="checkbox"/>	
DTIC TAB	<input type="checkbox"/>	
Unannounced	<input type="checkbox"/>	
Justification		
By		
Distribution/		
Availability Codes		
Dist	Avail and/or	Special
A-1		



**VIRGINIA
POLYTECHNIC
INSTITUTE
AND
STATE
UNIVERSITY**



REPRODUCED BY
NATIONAL TECHNICAL
INFORMATION SERVICE
U.S. DEPARTMENT OF COMMERCE
SPRINGFIELD, VA 22161

**BLACKSBURG,
VIRGINIA**

College of Engineering
Virginia Polytechnic Institute & State University
Blacksburg, Virginia 24061

VPI-E-82-9

April 1982

ON THE OFF-AXIS TENSILE TEST
FOR UNIDIRECTIONAL COMPOSITES

Michael P. Nemeth¹

Carl T. Herakovich²

Daniel Post²

Department of Engineering Science & Mechanics

Interim Report 28
The NASA-Virginia Tech Composites Program

NASA Cooperative Agreement NCCI-15
NSF Grant Eng-7824609

Prepared for: Materials Processing & Application Branch
National Aeronautics & Space Administration
Langley Research Center
Hampton, Virginia 23665
National Science Foundation
Washington, D. C. 20550

¹Graduate Student

²Professor

BIBLIOGRAPHIC DATA SHEET	1. Report No. VPI-E-82-9	2.	3. Recipient's Accession No. D892 203720
	4. Title and Subtitle ON THE OFF-AXIS TENSILE TEST FOR UNIDIRECTIONAL COMPOSITES		5. Report Date
7. Author(s) M. P. Nemeth, C. T. Herakovich, D. Post		8. Performing Organization Report No. VPI-E-82-9	
9. Performing Organization Name and Address Virginia Polytechnic Institute and State University Engineering Science and Mechanics Blacksburg, Virginia 24061		10. Project/Task/Work Unit No.	
12. Sponsoring Organization Name and Address National Aeronautics & Space Admin. National Science Found. Langley Research Center Washington, D. C. 20550 Hampton, Virginia 23665		11. Contract/Grant No. CA NCCI-15 and NSF Grant Eng-7824609	
15. Supplementary Notes		13. Type of Report & Period Covered	
16. Abstracts The off-axis tensile test was examined experimentally to obtain actual displacement fields over the surface of graphite-polyimide coupon specimens; the experimental results were compared with the approximate analytical solution of Pagano and Halpin and newly generated finite element results. A new optical method of high sensitivity moiré interferometry was used to determine the actual displacements to high precision. It is shown that the approximate analytical solution and the finite element results compare very favorably with the measured centerline displacements in the test section, and the finite element displacement fields provide excellent agreement with the moiré displacements throughout the specimen. Results are presented for a 15 degree fiber orientation and coupon aspect ratios of 5 and 15.		14.	
17. Key Words and Document Analysis. 17a. Descriptors composites, off-axis, moiré, finite elements, displacements, stresses, theory, experiment			
17b. Identifiers/Open-Ended Terms			
17c. COSATI Field/Group			
18. Availability Statement		19. Security Class (This Report) UNCLASSIFIED	21. No. of Pages
		20. Security Class (This Page) UNCLASSIFIED	22. Price

DWG QUALITY INSPECTED 2

INTRODUCTION

The off-axis tensile test [1-4] has received considerable attention as a basic test method for material characterization of fibrous composites. It has been used to verify the applicability of the tensor transformation equations for elastic properties, as a shear test method [5-8], and as a strength test [8-10]. A potentially advantageous feature of the test is the biaxial stress state in the material principal coordinates. This stress state is useful for studies on the influence of stress interaction on nonlinear behavior and strength. The biaxial stress state can be a disadvantage if the biaxial stresses are not known accurately or if they are not properly considered.

An important difficulty with the off-axis test is the extensional-shear coupling associated with the anisotropic material behavior of the coupon and the constraints of the test fixture. An analytical solution for the exact boundary value does not exist, but an approximate solution was proposed by Pagano and Halpin [1], and finite element results were presented in [2,3,5]. Indeed the "exact" boundary value problem to be studied cannot be stated with mathematical certainty because of possible specimen pull-out from the grips.

The experimental determination of elastic properties and nonlinear behavior of composite materials requires a zone of uniform strain in the test section. The off-axis coupon under fixed-grip loading results in a nonuniform strain distribution with rather severe gradients near the grips. However, finite element results and the approximate

solution of Pagano and Halpin predict that a region of uniform strain is attained in the central test section of the specimen if the aspect ratio is large enough. Full field displacements showing the high gradients near the grips and the influence of aspect ratio on the strain distribution in the central test section of the specimen have not previously been demonstrated experimentally for advanced composite materials. The rationale and objectives of this paper are

1. experimental determination of the full displacement field for off-axis loading of advanced composites;
2. demonstration of the influence of specimen aspect ratio;
3. evaluation of finite element solutions by comparison with experimentally generated displacement fields;
4. presentation of stress fields determined by finite element studies;
5. corroboration of the approximate analytical solution of Pagano and Halpin by agreement with experimentally generated lateral displacements of the centerline; and
6. demonstration of a powerful experimental measurement method.

BASIC CONSIDERATIONS

In order to qualitatively assess the influence of the extensional shear coupling on the off-axis test (Fig. 1), it is essential to note its dependence upon the coefficient of mutual influence

$\bar{\eta}_{xy,x} = \bar{S}_{16}/\bar{S}_{11}$ (where \bar{S}_{16} and \bar{S}_{11} are components of the compliance matrix) and the specimen aspect ratio $\lambda = L/W$. An approximate analytical expression for the error in axial modulus E_x was developed by Pagano and Halpin [1]. It is written here in an amended form

$$E_x^* = E_x \left(\frac{1}{1 - \beta} \right) \quad (1)$$

where

$$\beta = \frac{3\eta_{xy,x}^2}{3 \left(\frac{E_x}{G_{xy}} \right) + 2\lambda^2} \quad (2)$$

The coefficient β is a measure of the error between the apparent modulus E_x^* and the actual modulus E_x . The error approaches zero as $\eta_{xy,x} \rightarrow 0$ or as $\lambda \rightarrow \infty$. The ratio E_x/G_{xy} is finite and decreases with increasing θ ($0 \leq \theta \leq 90$). As indicated in Fig. 2, $\eta_{xy,x}$ has a maximum critical value at approximately $\theta = 10^\circ$ for the material under consideration (Table 1). The coefficient of mutual influence is a material coefficient, whereas β is a function of material properties, specimen geometry and assumptions of the approximate solution.

Figure 3 shows the variation of β with fiber orientation θ and aspect ratio λ . For aspect ratios in the range 2-15, the critical fiber angle ranges from 17-10 degrees with a maximum value $\beta = 0.420$ for $\lambda = 2$ and $\theta = 17^\circ$. In contrast, for $\lambda = 15$, $\beta_{\max} = 0.037$ at $\theta = 10$ degrees. Figure 3 shows that the approximate solution of Pagano and Halpin predicts that the extensional-shear coupling effects can be significant over a range of fiber orientations depending upon specimen aspect ratio. The effect of this undesirable coupling on the determination of the axial modulus can be made negligibly small through the use of specimens with large aspect ratios. Using Figs. 2 and 3 as a guide, the authors chose to investigate the 15 degrees off-axis coupon in greater detail.

MOIRÉ ANALYSIS

An experimental investigation was undertaken to enable comparison with and evaluation of the approximate results. The specimen was unidirectional HTSi/PMR-15 graphite-polyimide. Two specimens with aspect ratios of 5 and 15 were machined to the dimensions shown in Fig. 4. The fiber orientation was 15 degrees from the longitudinal axis.

The specimens were clamped along the enlarged end sections in a tensile loading fixture which had a precision guided head. The fixture ensured pure longitudinal translation, i.e. fixed-grip displacement loading conditions.

A new optical method of high-sensitive moiré interferometry was used. The method gives the in-plane displacements throughout the field of view. Specifically, it reveals interference fringe patterns that are contours of constant U and V displacements, where U and V are the in-plane longitudinal and lateral displacements, respectively. Sensitivity was 32.8×10^{-6} in. per fringe ($0.833 \mu\text{m}/\text{fr}$); since interpolation to a fraction of a fringe is normal, displacements are determined with an accuracy of a few microinches.

The method utilized a thin cross-line diffraction grating of silicone rubber on the surface of the specimen. Frequency of the specimen grating was 15,240 lines per inch ($600 \text{ } \ell/\text{mm}$). A virtual reference grating of 30,480 $\ell/\text{in.}$ ($1200 \text{ } \ell/\text{mm}$) was superimposed on the specimen grating by a simple optical system. The specimen grating deformed together with the specimen as tensile loads were applied and moiré interference fringes were formed by the interaction of the deformed

specimen grating and the undeformed reference grating.

The moiré method is described in detail in [11,12]. Actually, the test example used in [11] to demonstrate the technique was nearly the same as the specimens studied here. However, rigid grip loading conditions were not achieved sufficiently well in that work and the specimens and loading fixture were refined for the present study.

FINITE ELEMENT ANALYSIS

In an effort to further evaluate the off-axis test, the fixed-grip displacement loading condition was investigated numerically using the finite element method. This loading condition is the idealized model of the test described in the section on moiré analysis. More specifically, a displacement formulation for plane stress anisotropic elasticity was used. To increase the numerical accuracy and eliminate any preferential direction in the response, rectangular elements composed of four constant strain triangles were used in conjunction with static condensation to eliminate the internal nodes. The two meshes used in the present study contained 861 nodes and 800 elements. Results were obtained for aspect ratios of 5 and 15 for the 15° off-axis angle.

RESULTS AND DISCUSSION

Theoretical/Experimental Comparisons

The U and V displacement fields from a finite element analysis of one-half the specimen are shown along with the moiré results in Figs. 5 and 6. Practically constant fringe orders along the top of each moiré pattern confirms the good approximation to the fixed grip

conditions in the test; further study confirms nearly zero lateral motion at the grips. A high strain concentration in one corner of the coupon with aspect ratio of 5 is also evident. The moiré interferometry patterns define the displacement fields for these physical specimens with high precision.

Comparison of these figures indicates very good correlation between theory and experiment. It is concluded from these figures that the fixed-end finite element solution is a good representation of the actual displacement field.

Results for the centerline lateral displacements obtained using moiré, finite elements and the Pagano and Halpin solutions are compared in Figs. 7 and 8. A unifying condition was imposed to calculate lateral displacements, namely, the centerline longitudinal displacement was made equal to that of the real specimen in each case. These figures show that there is very good agreement between all three methods of analysis. The finite element solution provides better results for the maximum lateral deflection for the larger aspect ratio and the approximate solution provides better agreement for the smaller aspect ratio. However, the difference in actual displacements is very small in all cases. There is no significant difference in slopes (i.e. strain). As expected, the fully constrained finite element model always predicts larger lateral displacements than the less constrained solution of Pagano and Halpin. Comparison of the two figures shows that there is very little difference in the actual lateral displacement for the aspect ratios of 5 and 15.

The influence of aspect ratio is more clearly demonstrated in Fig. 9 which shows plots of the lateral displacements of the Pagano and Halpin solution normalized with respect to specimen width. For a threefold increase in aspect ratio there is a threefold increase in the maximum normalized lateral displacement.

A comparison of displacements along the specimen quarter points (widthwise) shows that the finite element solution is more accurate near the grips (Fig. 10). It is not expected that the Pagano and Halpin solution would provide good agreement in this region as boundary conditions were specified only on the centerline.

It is also evident from results of the finite element analysis in Figs. 11-13 that a complex biaxial stress state with high stress concentrations is present in one corner of the specimen. The lack of exact satisfaction of stress boundary conditions in these figures is typical of finite element results obtained using constant stress elements and is not a serious problem. The contours were plotted by computer with contour values chosen to exhibit the magnitude of the stress concentrations in the corners; this also contributed to the apparent lack of satisfaction of boundary conditions.

The only assumption in the Pagano and Halpin solution is that the shear stress is independent of longitudinal coordinate. (All displacement boundary conditions in their solution are consistent with the actual displacements.) Having shown that the finite element solution provides a very good approximation to the actual displacement field (Figs. 5-7), we can determine the extent to which this assumption on stress is valid from the finite element results. Contours of shear

stress for aspect ratios of 5 and 15 are shown in Fig. 12. While there is some variation in shear stress along the centerline it is not severe. Indeed, in the central portion of the specimen (gage section) the shear stress is independent of the axial coordinate. There is a rather severe stress concentration in one corner. The larger aspect ratio provides a larger region of uniform stress as well as lower transverse and shear stress in the test section. The Pagano and Halpin solution predicts zero transverse stress throughout the specimen. The finite element results show that this condition is approached as the specimen aspect ratio is increased.

Factors Influencing Theoretical/Experimental Comparisons

In any attempt to make a precise correlation between theory and experiment there will be some aspects of the problem which will not be identical in both analyses. Some of those which may have had an effect on the current study are discussed in this section. The engineering properties used in the theoretical solutions were based upon test results from material of the same specification, but a different batch than that used for these experimental tests. Pure shear test results were not available; hence, it was necessary to estimate G_{12} based on results from a $[\pm 45]_s$ tensile test and other investigations of shear modulus obtained from off-axis tests [7,8]. (As will be shown, lateral displacement of the coupon is sensitive to G_{12} .) An acceptable moiré grid could be established only to within 0.04 in. (1 mm) of the actual specimen end. The displacements at the "exact" end of the specimen were determined by extrapolation of the moiré results. Also,

the properties and thickness of the actual specimen may vary slightly from point to point. Finally, both approximate solutions assumed linear elastic behavior everywhere. There is a strong possibility that the shear behavior, in particular, is nonlinear in the corner with the high stress concentrations. For these reasons, exact equality of experimental and theoretical results should not be expected and engineering judgement must be exercised.

The influence of the shear modulus on the lateral deflection of the specimen centerline is clearly shown in Fig. 14 where the Pagano and Halpin solution was used to present results for a range of shear modulus values. It is observed that the maximum deflection varies by as much as twenty-five percent for shear moduli ranging from $0.6 - 1.0 \times 10^6$ psi. The lower value corresponds to that obtained from a $[\pm 45]_5$ tensile test [13] and the higher value corresponds more closely to off-axis tensile and rail shear tests for similar materials [7,8]. Based upon these results a value of $G_{12} = 0.725 \times 10^6$ psi was used for the theoretical predictions in the comparisons between theory and experiment.

CONCLUSIONS

High precision experimental results have been presented for the full-field displacements of unidirectional off-axis graphite-polyimide coupons. The experimental results show the existence of high strain gradients near the grips, and the influence of specimen aspect ratio on the displacement field. Excellent correlation between experimental and

finite element results is shown for the entire displacement field.

The approximate analytical solution of Pagano and Halpin is shown to be quite accurate in the central test section of the specimen. The accuracy of the approximate solution increases with increasing aspect ratio. It is recommended that aspect ratios of 15 or larger be used for determination of elastic constants.

The results of this investigation verify the existence of strain and stress concentrations in two corners of the specimen. These stress concentrations are not predicted by the approximate analytical solution and hence finite element analysis is preferred for studies on strength.

REFERENCES

1. Pagano, N. J., and Halpin, J. C., "Influence of End Constraints in the Testing of Anisotropic Bodies," Journal of Composite Materials, Vol. 2, No. 1, 1968, p. 18-31.
2. Rizzo, R. R., "More on the Influence of End Constraints on Off-Axis Tensile Tests," Journal of Composite Materials, Vol. 3, 1969, p. 202-219.
3. Richards, G. L., Airhart, T. P., and Ashton, J.E., "Off-Axis Tensile Coupon Testing," Journal of Composite Materials, Vol. 3, 1969, p. 586-589.
4. Wu, E. and Thomas R., "Note on the Off-Axis Test of a Composite," Journal of Composite Materials, Vol. 2, 1968, p. 523.
5. Chamis, C. C. and Sinclair, J. H., "Ten-degree Off-Axis Test for Shear Properties in Fiber Composites," Experimental Mechanics, Vol. 17, No. 9, Sept. 1977, p. 339.
6. Chiao, C. C., Moore, R. L. and Chiao, T. T., "Measurement of Shear Properties of Fiber Composites. Part 1 Evaluation of Test Methods," Composites, July 1977, p. 161.
7. Yeow, Y. T. and Brinson, H. F., "A Comparison of Simple Shear Characterization Methods for Composite Laminates," Composites, January 1978, p. 49.
8. Pindera, M. J. and Herakovich, C. T., "An Endochronic Theory for Transversely Isotropic Fibrous Composites," VPI-E-81-27, Virginia Polytechnic Institute and State University, Blacksburg, Oct. 1981.
9. Pipes, R. B. and Cole, B. W., "On the Off-Axis Strength Test for Anisotropic Materials," Journal of Composite Materials, Vol. 7, April 1973, p. 246.
10. Kim, R. Y., "On the Off-Axis and Angle Ply Strength of Composites," Test Methods and Design Allowables for Fibrous Composites, ASTM STP 734, C. C. Chamis, Ed., Am. Soc. Testing & Materials, 1981, p. 91-108.
11. Post, D. and Baracat, W. A., "High-Sensitivity Moiré Interferometry - A Simplified Approach," Experimental Mechanics. Vol. 21, No. 3, March 1981, p. 100.
12. Post, D., "Developments in Moiré Interferometry," Optical Engineering (to be published May 1982).

13. Shuart, M. J., and Herakovich, C. T., "An Evaluation of the Sandwich Beam in Four-Point Bending as a Compressive Test Method for Composites," NASA TM 78783, Sept. 1978.

TABLE 1
ELASTIC PROPERTIES OF HTS1/PMR-15 GRAPHITE-POLYIMIDE

$$E_1 = 18.7 \times 10^6 \text{ psi}$$

$$\nu_{12} = 0.34$$

$$E_2 = 1.19 \times 10^6 \text{ psi}$$

$$G_{12} = 0.72 \times 10^6 \text{ psi}$$

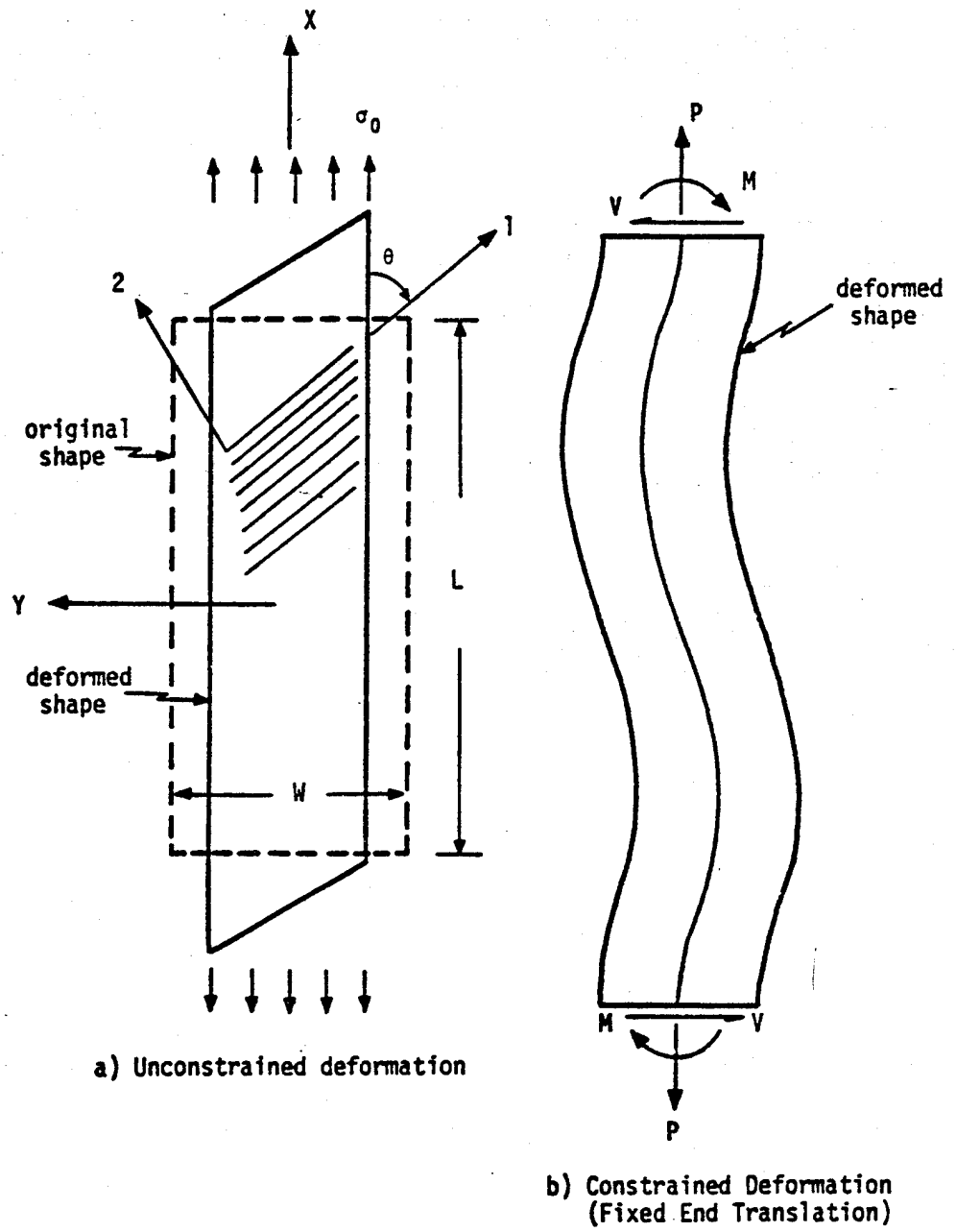


Fig. 1 Deformation Modes of Off-Axis Tensile Coupon

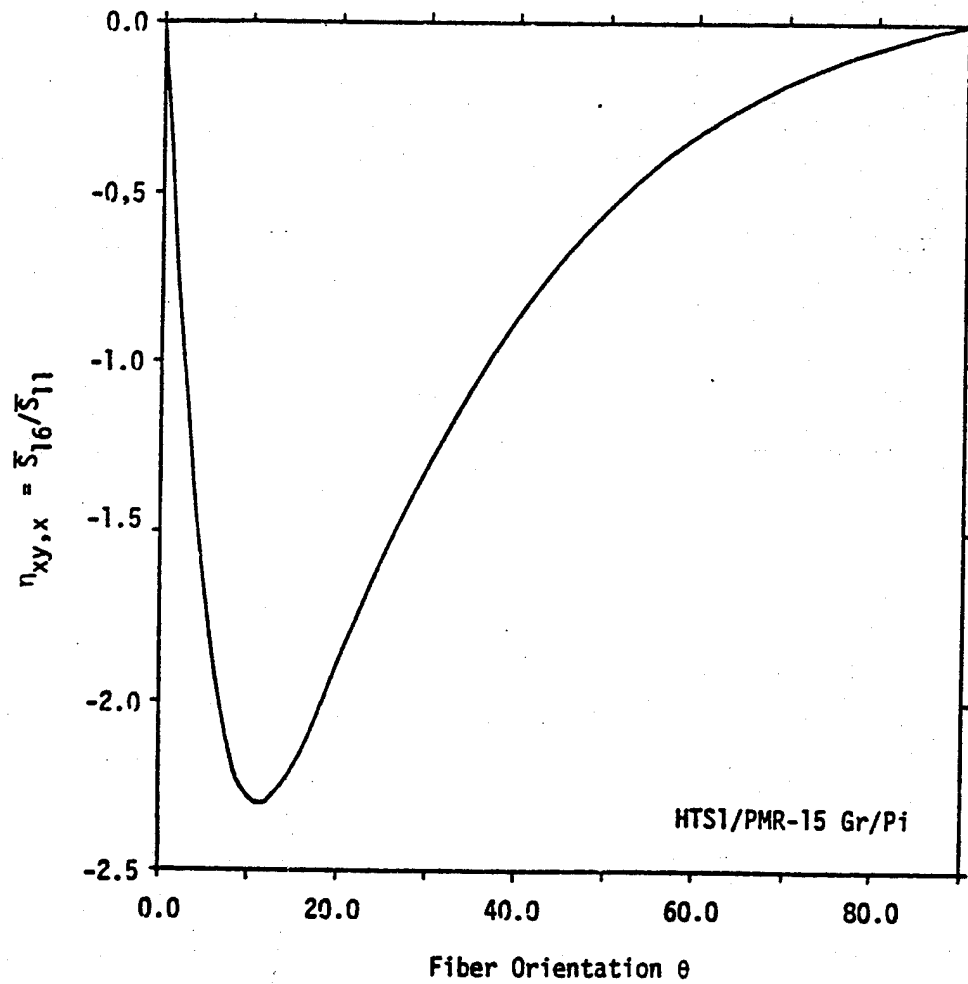


Fig. 2 Coefficient of Mutual Influence $\eta_{xy,x}$

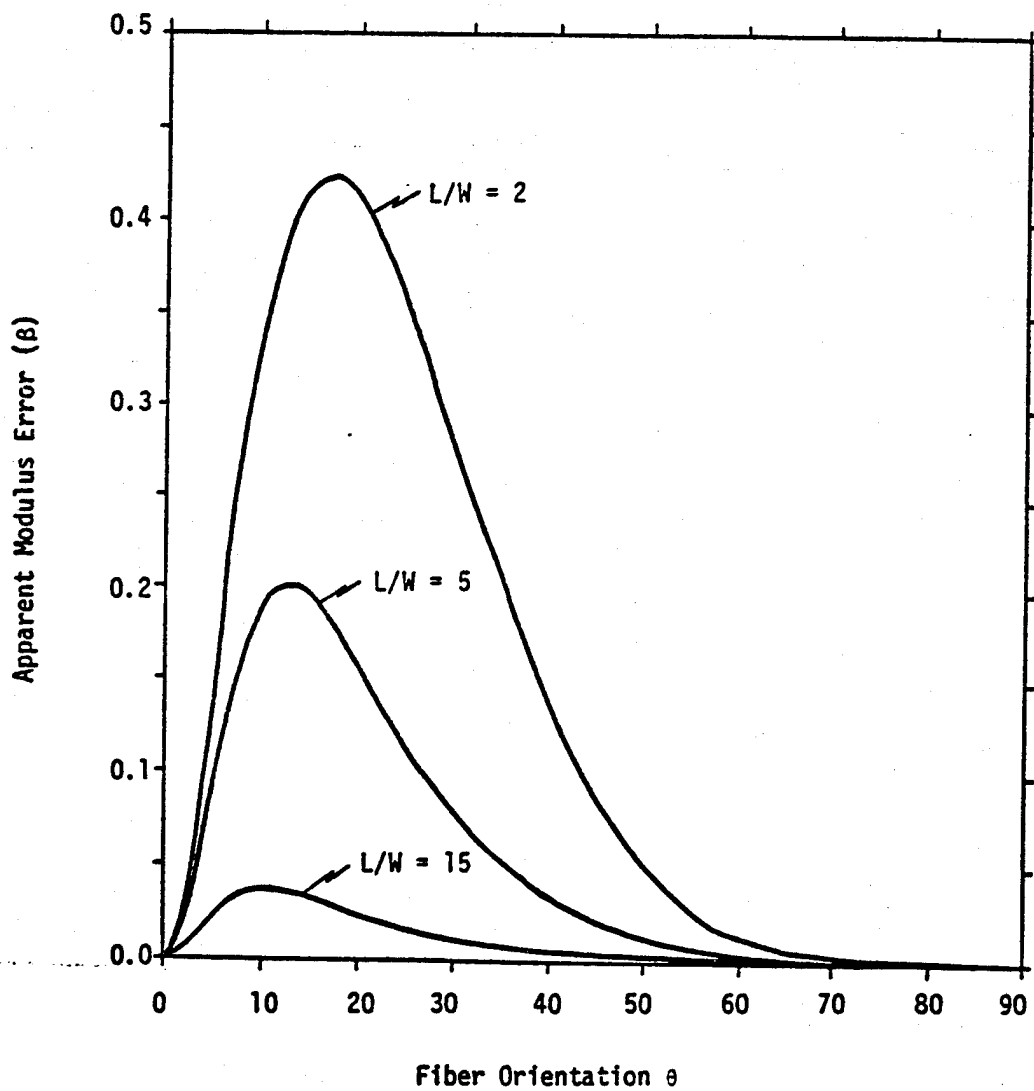
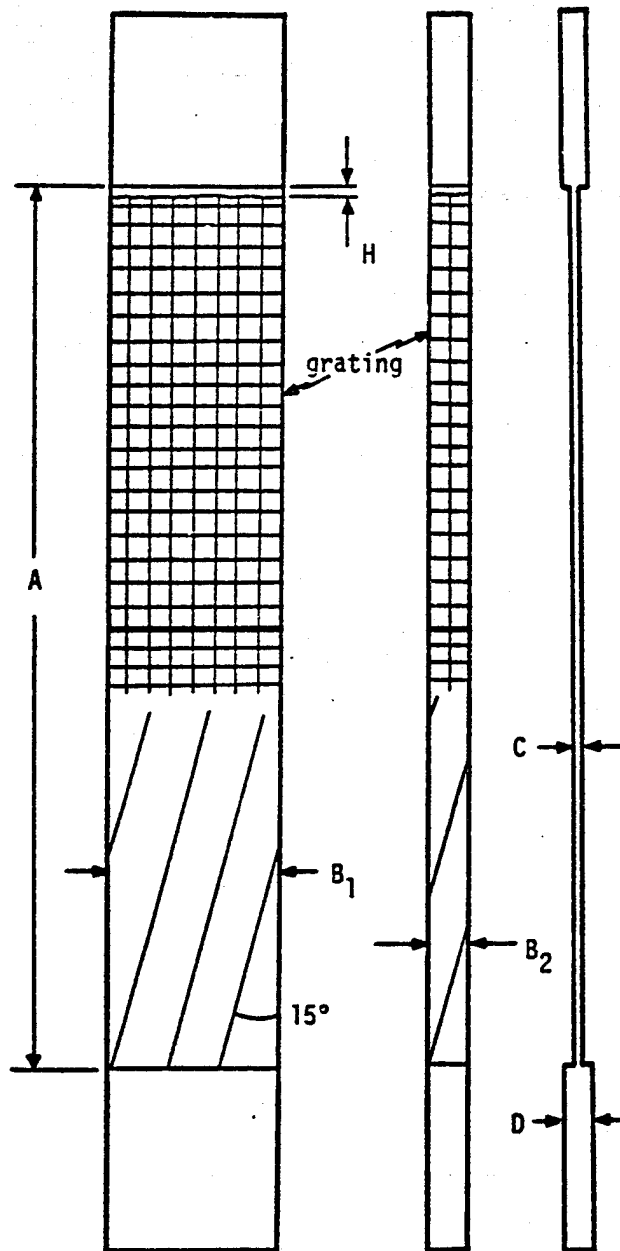


Fig. 3 Apparent Modulus Error (β) for HT51/PMR-15 Graphite Polyimide, based upon Approximate Solution of Pagano and Halpin [1].



	<u>in</u>	<u>mm</u>
A	4.00	102
B ₁	0.800	20.3
B ₂	0.267	6.76
C	0.012	0.30
D	0.048	1.2
H	0.04	1

Fig. 4 Test Specimens

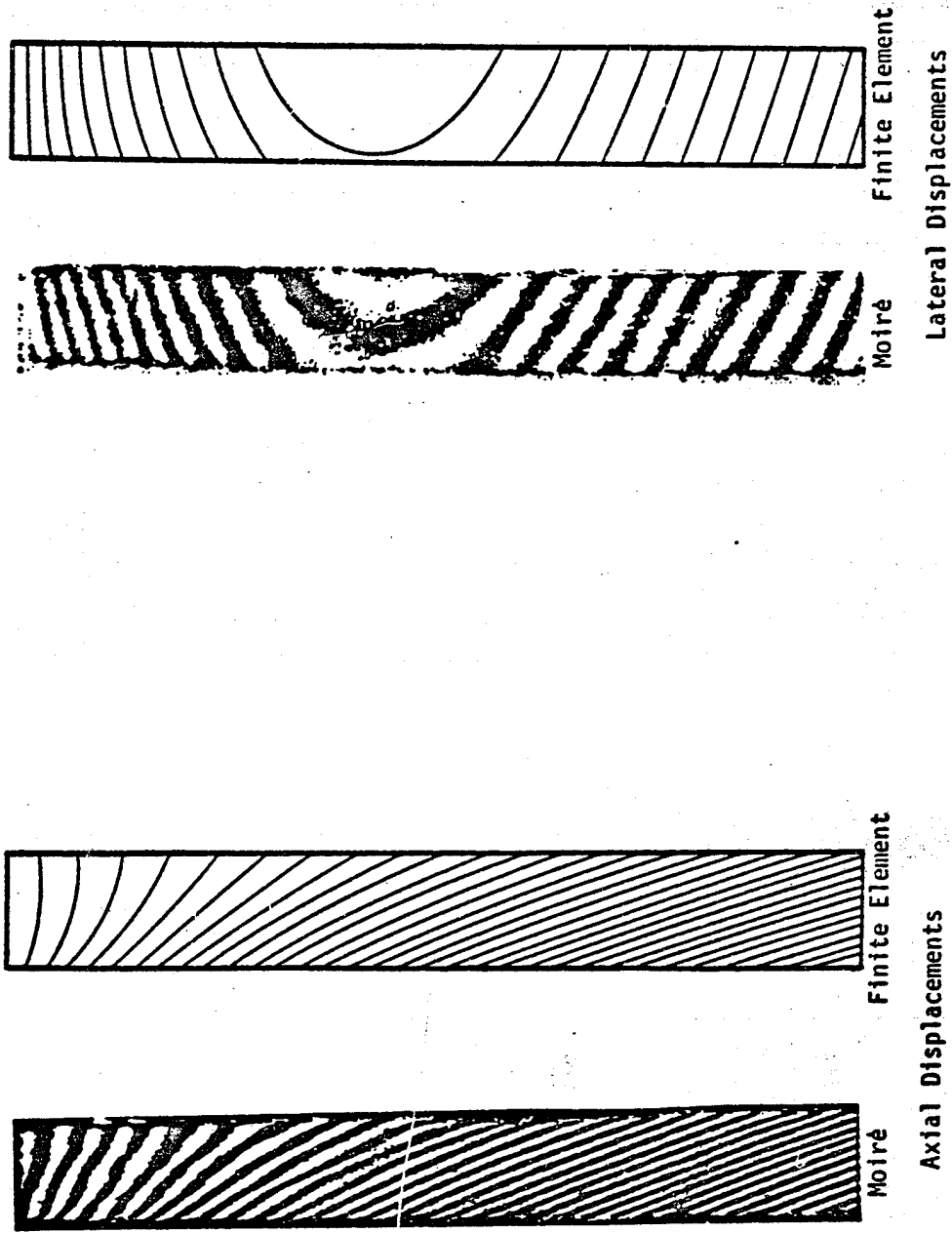
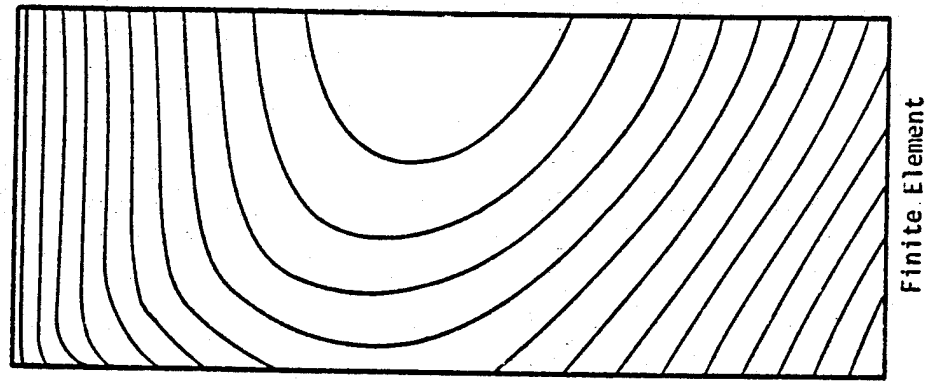


Fig. 5 Moiré and Finite Element Displacement Fields ($L/M = 15$)

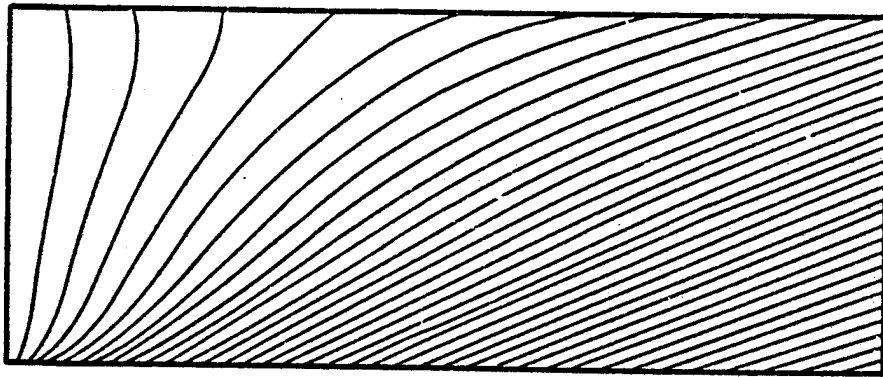


Finite Element

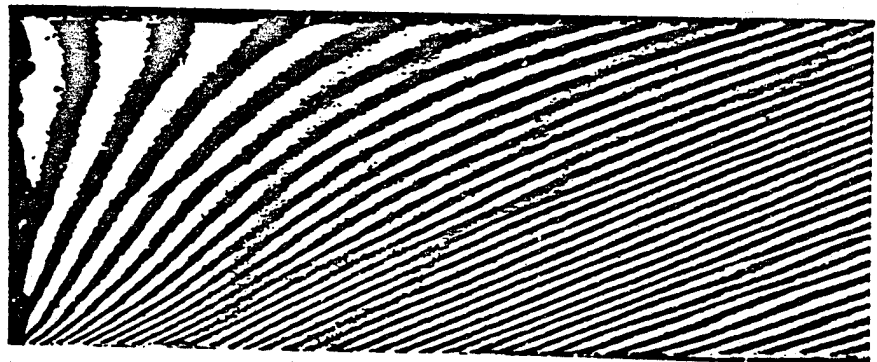


Moiré

Lateral Displacements



Finite Element



Moiré

Axial Displacements

Fig. 6 Moiré and Finite Element Displacement Fields ($L/W = 5$)

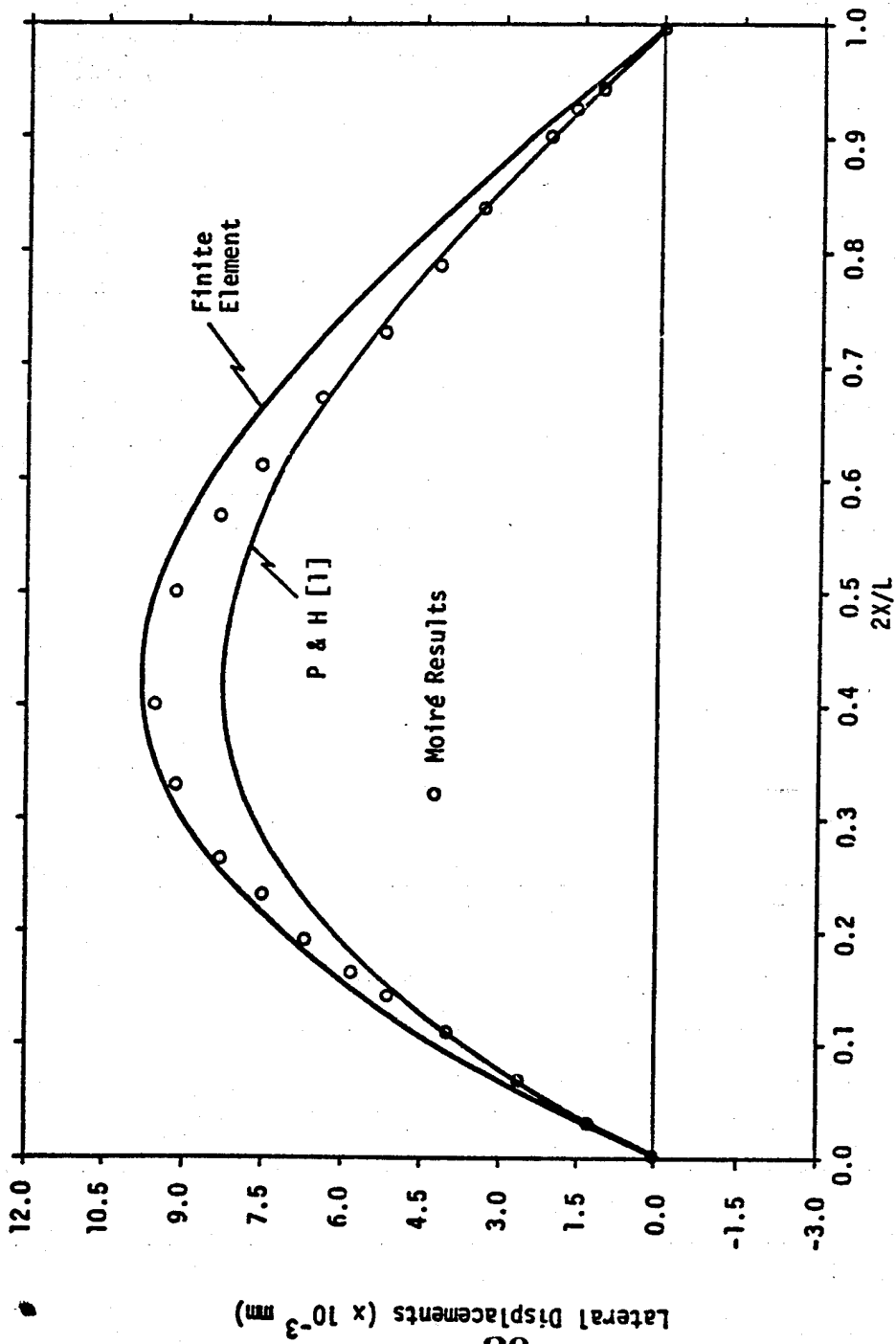


Fig. 7 Comparison of Centerline Lateral Displacement for $L/W = 15$

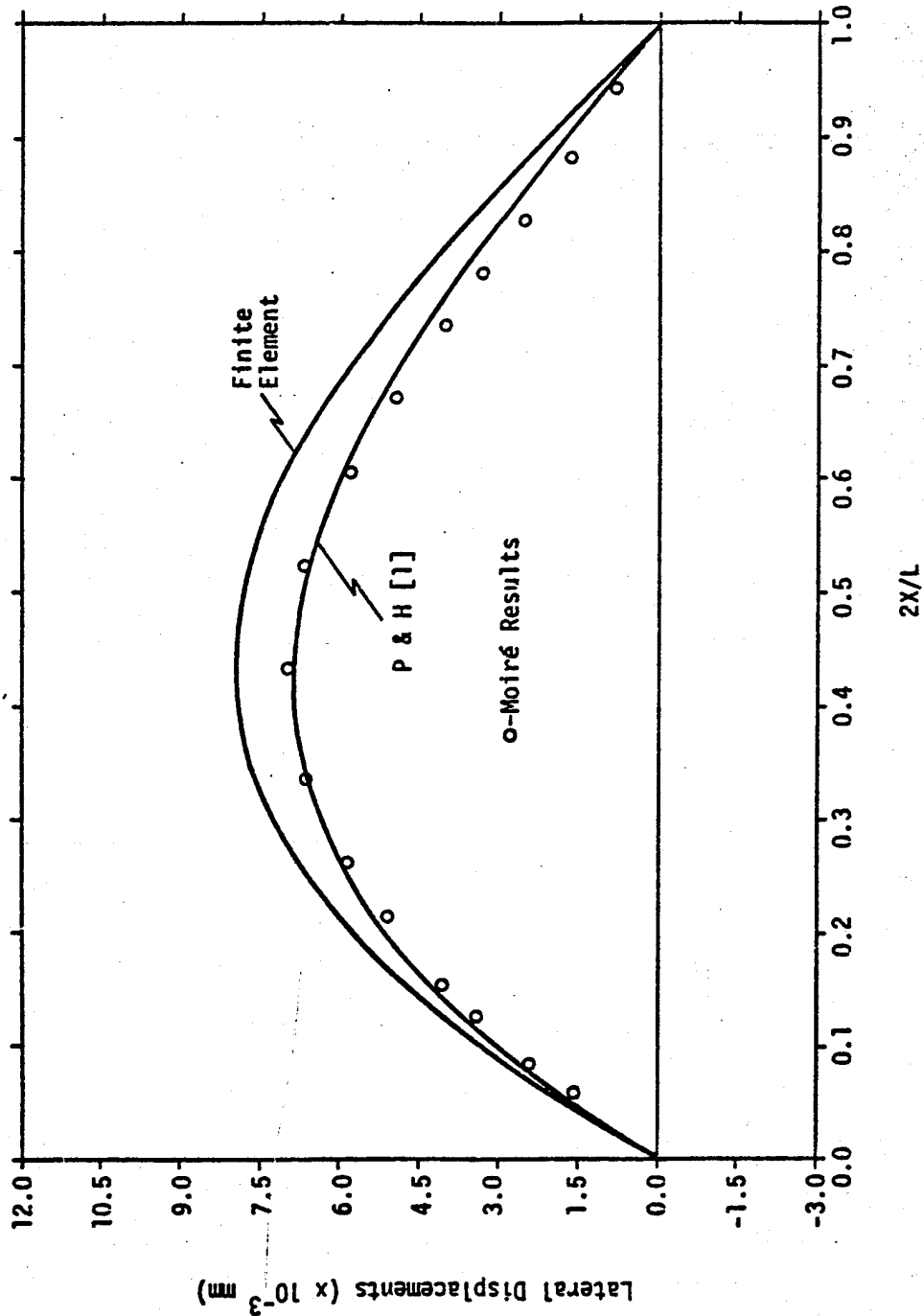


Fig. 8 Comparison of Centerline Lateral Displacements for $L/W = 5$

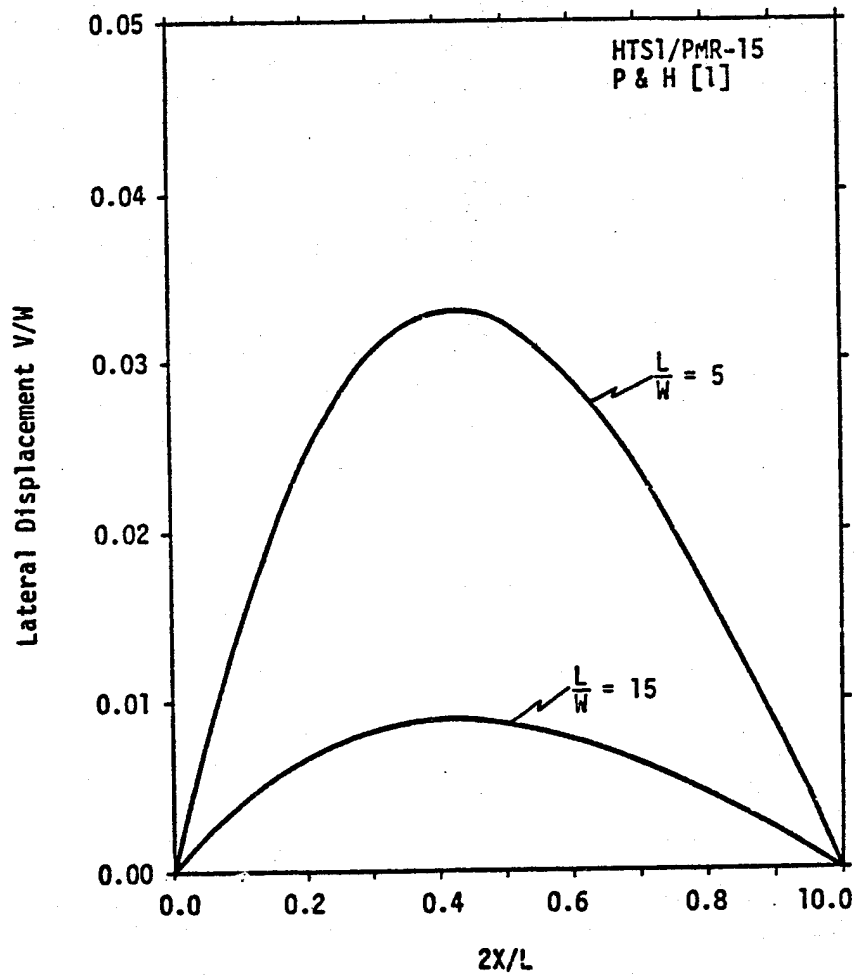


Fig. 9 Normalized Centerline Lateral Displacements

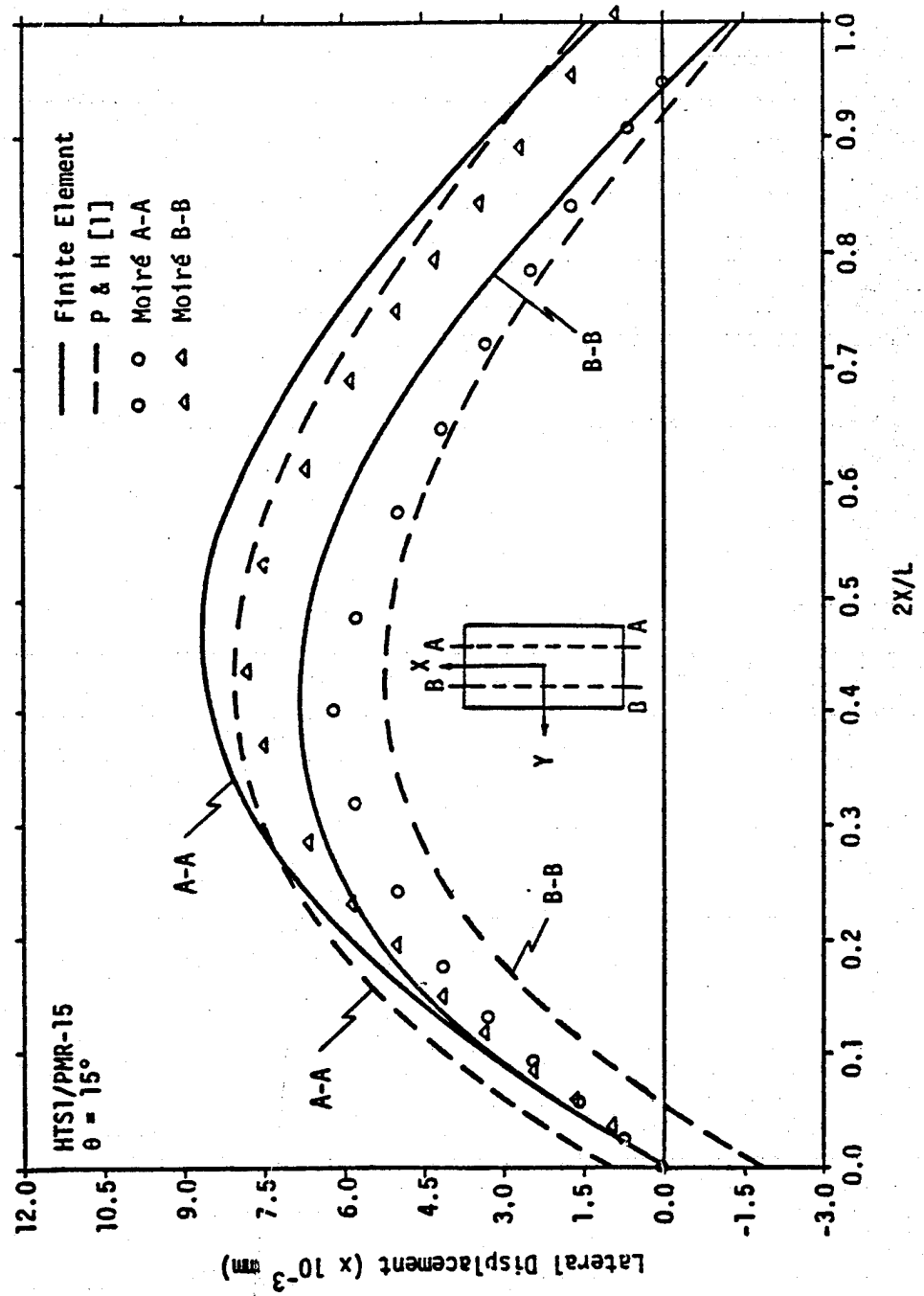


Fig. 10 Displacements Along Quarter Points ($L/W = 5$)

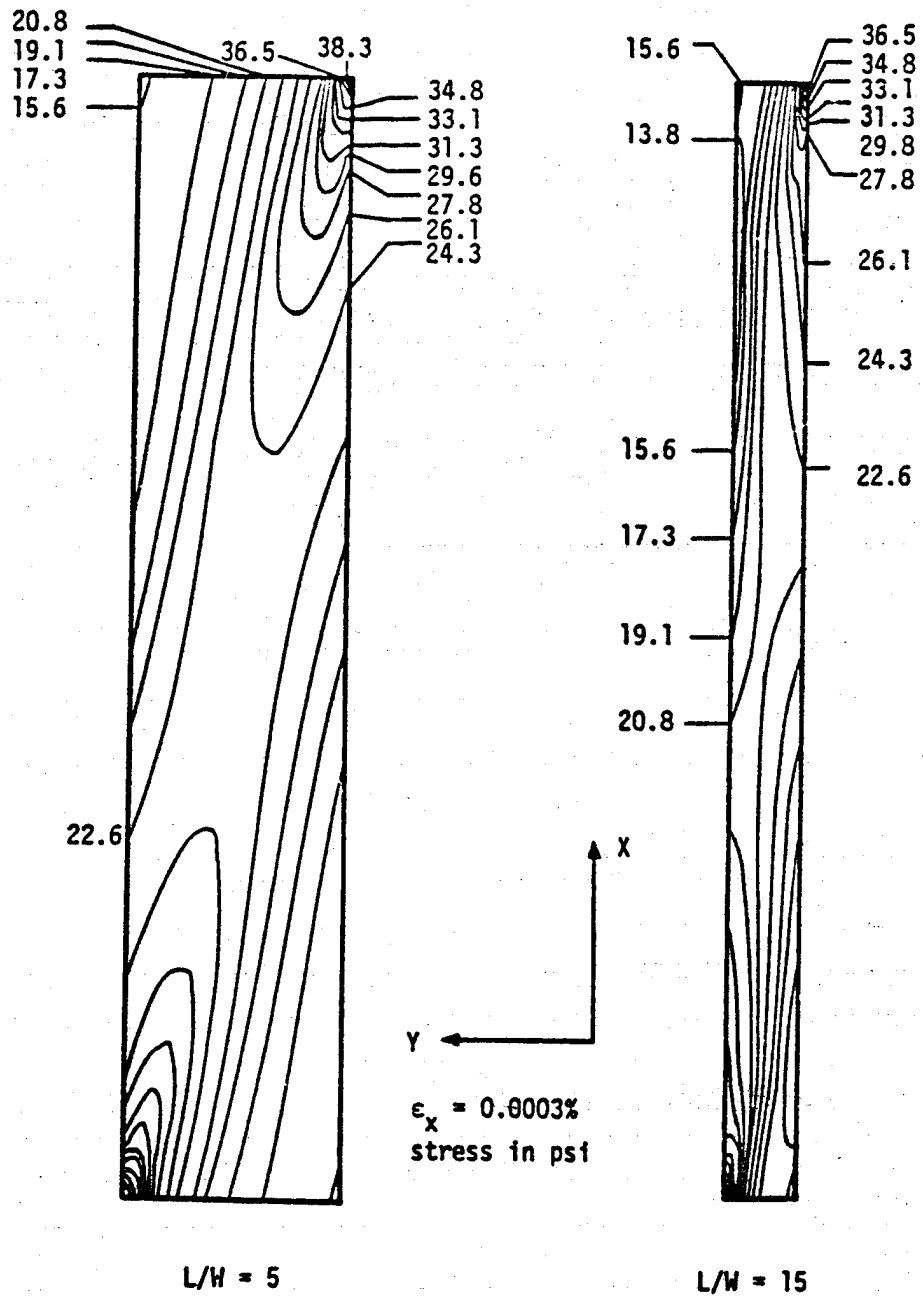


Fig. 11 σ_x Stress Contours for 15° Off-Axis Tensile Coupons

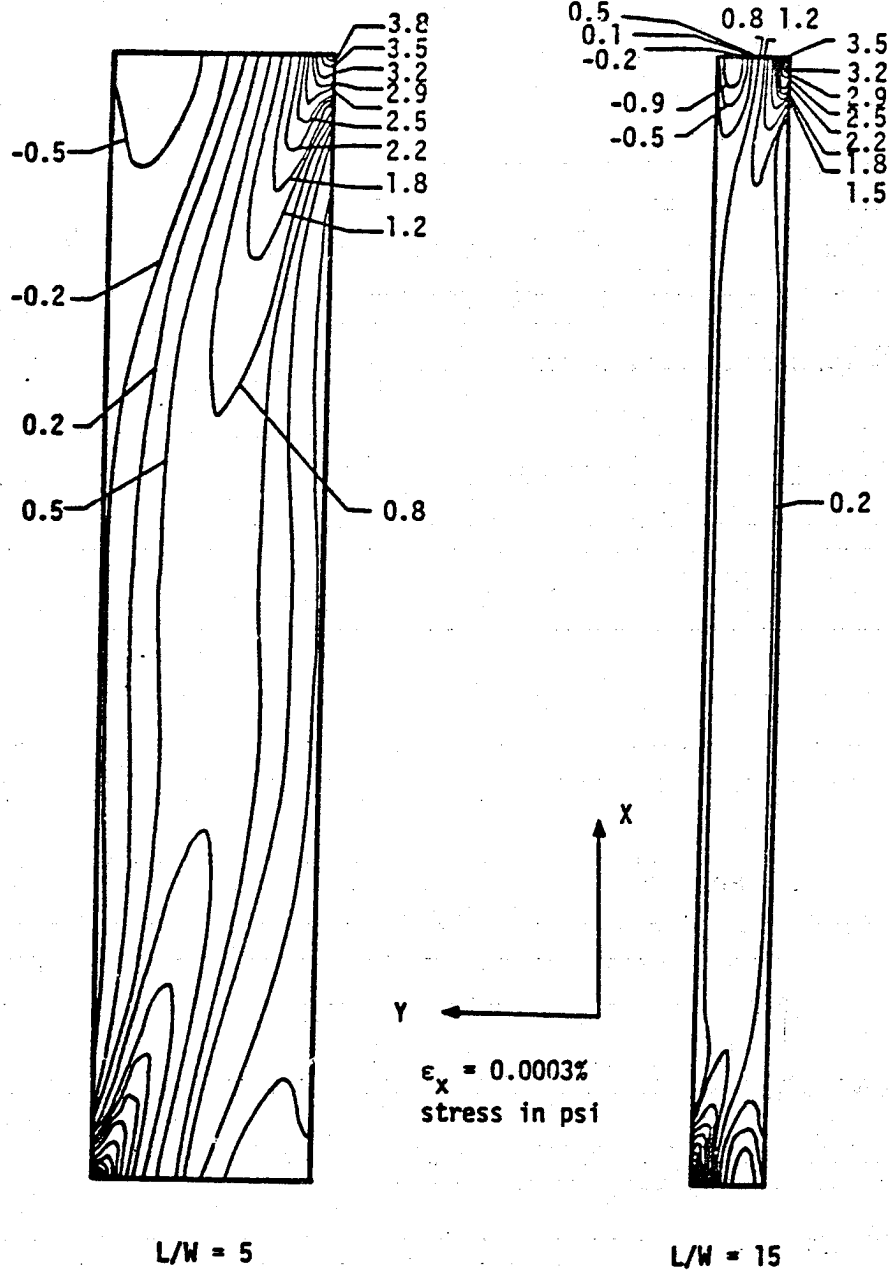


Fig. 12 τ_{xy} Stress Contours for 15° Off-Axis Gr/Pi Tensile Coupons

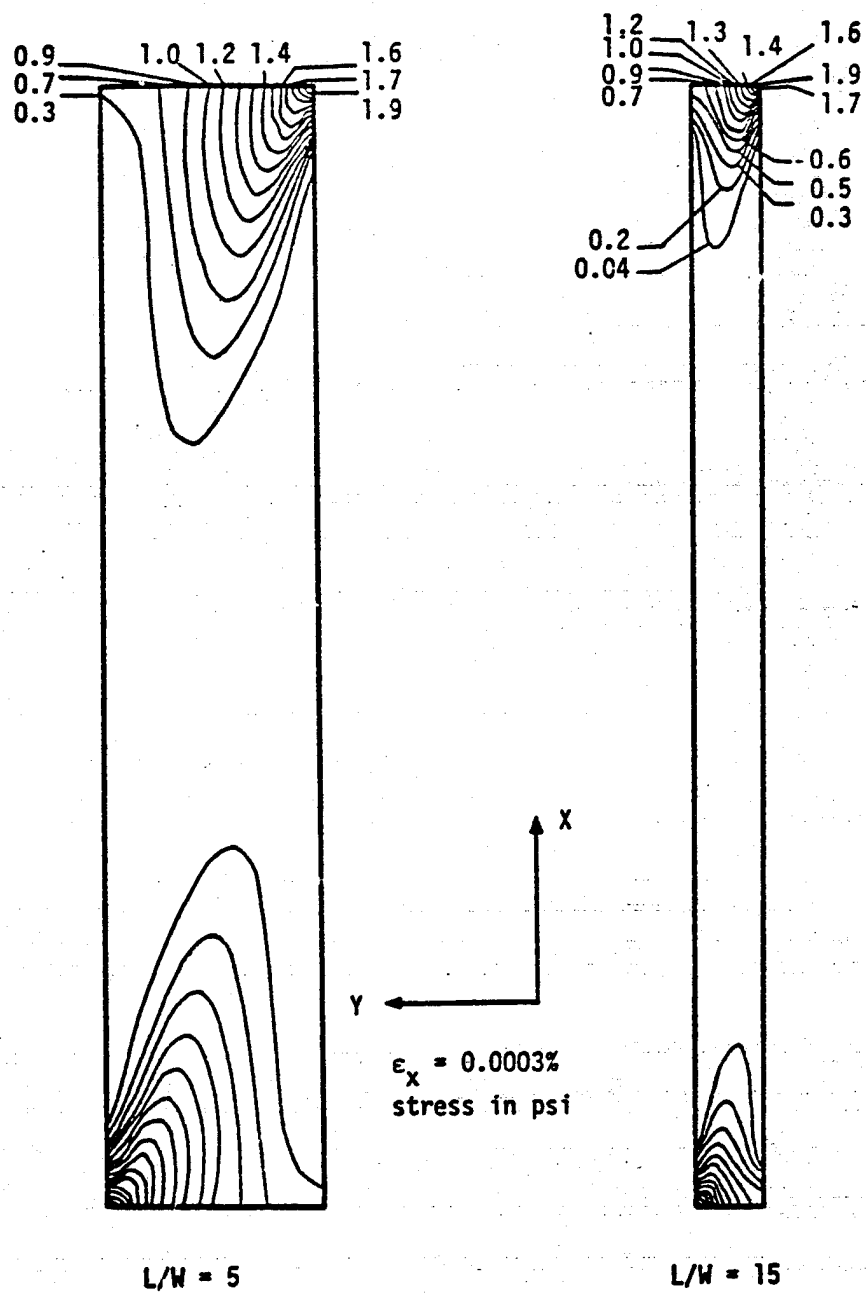


Fig. 13 σ_y Stress Contours for 15° Off-Axis Tensile Coupons

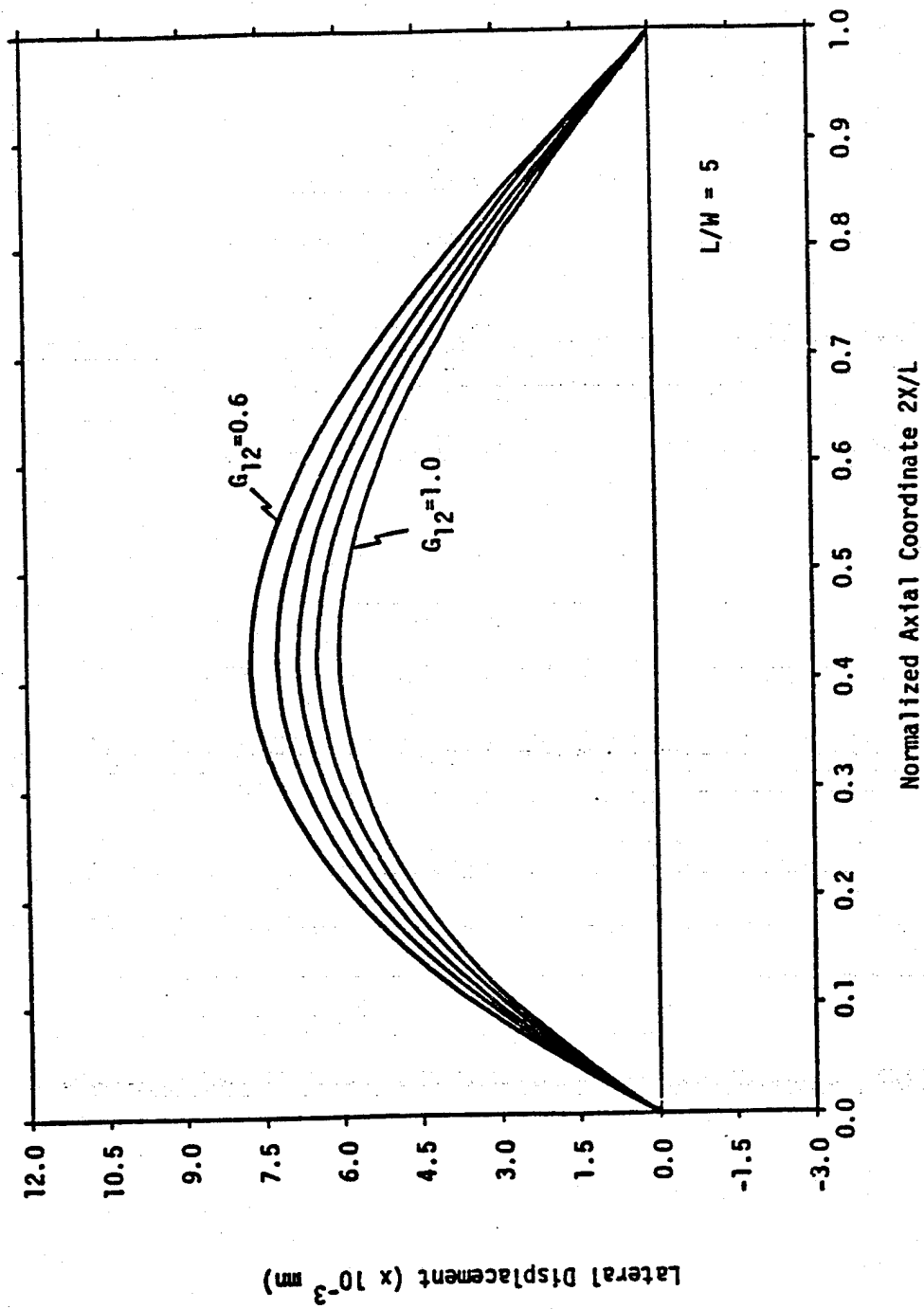


Fig. 14 Influence of Shear Modulus on Centerline Lateral Displacement of Off-Axis Tensile Coupon

END
DATE
FILMED
7-16-82
NTIS